Front. Environ. Sci. Eng. 2023, 17(5): 62
https://doi.org/10.1007/s11783-023-1662-8

RESEARCH ARTICLE

Identify the contribution of vehicle non-exhaust emissions: a single particle aerosol mass spectrometer test case at typical road environment

Qijun Zhang[1], Jiayuan Liu[1], Ning Wei[1], Congbo Song[2], Jianfei Peng[1], Lin Wu (✉)[1], Hongjun Mao (✉)[1]

1 Tianjin Key Laboratory of Urban Transport Emission Research & State Environmental Protection Key Laboratory of Urban Ambient Air Particulate Matter Pollution Prevention and Control, College of Environmental Science and Engineering, Nankai University, Tianjin 300071, China
2 School of Geography Earth and Environment Sciences, University of Birmingham, Birmingham B15 2TT, UK

HIGHLIGHTS

- A single particle observation was conducted in a high traffic flow road environment.
- Major particle types were vehicle exhausts, coal burning, and biomass burning.
- Contribution of non-exhaust emissions was calculated via PMF.
- Proportion of non-exhaust emissions can reach 10.1 % at road environment.

ARTICLE INFO

Article history:
Received 2 July 2022
Revised 6 September 2022
Accepted 14 October 2022
Available online 20 December 2022

Keywords:
Non-exhaust emissions
SPAMS
PMF
Roadside environment

GRAPHIC ABSTRACT

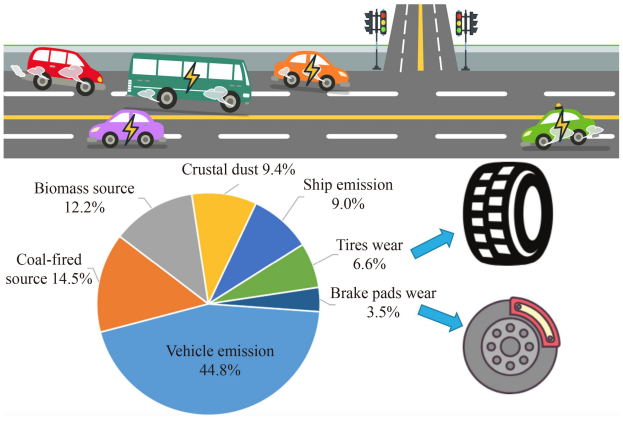

ABSTRACT

A single particle aerosol mass spectrometer (SPAMS) was used to accurately quantify the contribution of vehicle non-exhaust emissions to particulate matter at typical road environment. The $PM_{2.5}$, black carbon, meteorological parameters and traffic flow were recorded during the test period. The daily trend for traffic flow and speed on TEDA Street showed obvious "M" and "W" characteristics. 6.3 million particles were captured via the SPAMS, including 1.3 million particles with positive and negative spectral map information. Heavy Metal, High molecular Organic Carbon, Organic Carbon, Mixed Carbon, Elemental Carbon, Rich Potassium, Levo-rotation Glucose, Rich Na, SiO_3 and other categories were analyzed. The particle number concentration measured by SPAMS showed a good linear correlation with the mass concentrations of $PM_{2.5}$ and BC, which indicates that the particulate matter captured by the SPAMS reflects the pollution level of fine particulate matter. EC, ECOC, OC, HM and crustal dust components were found to show high values from 7:00–9:00 AM, showing that these chemical components are directly or indirectly related to vehicle emissions. Based on the PMF model, 7 major factors are resolved. The relative contributions of each factor were determined: vehicle exhaust emission (44.8 %), coal-fired source (14.5 %), biomass combustion (12.2 %), crustal dust (9.4 %), ship emission (9.0 %), tires wear (6.6 %) and brake pads wear (3.5 %). The results show that the contribution of vehicle non-exhaust to particulate matter at roadside environment is approximately 10.1 %. Vehicle non-exhaust emissions are the focus of future research in the vehicle pollutant emission control field.

✉ Corresponding authors
E-mails: wulin@nankai.edu.cn (L. Wu);
hongjunm@nankai.edu.cn (H. Mao)

1 Introduction

With the gradual relocation of industrial pollution sources to surrounding suburbs, the contribution rate of vehicle emissions in central urban areas is even higher. The particulate matter emitted by vehicles can be mainly divided into two categories: exhaust emissions and non-exhaust emissions. With the improvement of vehicle exhaust control measures and emission reduction technologies, the emission of vehicle exhaust has gradually been effectively controlled. At the same time, with the changes in the policy orientation of the world's major countries, major vehicle manufacturers have announced timetables for the suspension of traditional fuel vehicles. Therefore, it is foreseeable that the proportion of motor vehicle exhaust emissions will continue to decrease in the future, while non-exhaust emissions (brake pad wear and tire wear, etc.) will gradually increase. At present, the particulate matter of non-exhaust emission is not controlled by legislation. However, with the reduction in exhaust particulate matter emissions and the promotion of electric vehicles, research into non-exhaust particulate matter emissions has become important (Timmers and Achten, 2016).

At present, considerable studies have been conducted on vehicle exhaust emissions (Yue et al., 2012; Masclans Abello et al., 2021; Zhu et al., 2021). However, there are relatively few studies on vehicle non-exhaust particulate matter. The vehicle non-exhaust particulate matter mainly includes brake pad wear particulate matter and tire wear particulate matter (Kwak et al., 2013; Pant and Harrison, 2013; Amato et al., 2014; Baensch-Baltruschat et al., 2020; Pratico and Briante, 2020). Brake pad wear particles are mainly generated from the brake liner and brake disc or brake drum friction. Laboratory simulation is the most commonly used method for carrying out brake pad wear experiments. On the brake experimental platform, wear particles are collected via continuous friction between the experimental brake lining and brake disc or brake drum (Beddows et al., 2016). The key components of brake pads include fillers, friction additives, reinforcing fibres and adhesives. Key chemicals in brake pads include metal sulphides, abrasive agents (SiO_2), barium silicate/sulphate (especially brake liners), and other metal particles (fibre materials), carbon fibre, and lubricants (graphite). Grieshop et al. (2006) detected a higher concentration of particulate matter during high volume traffic (vehicles usually operating in a stop-and-go mode). Abu-Allaban et al. (2003) found that the contribution rate of brake wear at the exit of an expressway is higher than that in other roadside environments that do not require frequent braking, indicating that the particles released during the braking phase are much greater than those released during the acceleration phase (Mathissen et al., 2011). Gasser et al. (2009) found that the concentrations of Fe, Cu and organic carbon (OC) in the particulates emitted by different braking methods are high. Garg et al. (2000) found that metal elements account for 72 % of PM_{10} on average, with higher Fe, Cu, Ti, S, and Zr contents. Roubicek et al. (2008) tested brake pads produced in different regions and found that samples from Europe and Japan contained Sb_2S_3. Sb_2S_3 is an important lubricant for brake pads. It can reduce brake pad vibration and improve friction stability. Sb_2S_3 can be oxidized to Sb_2O_3 during braking and has been classified as a potential carcinogen (Von Uexkull et al., 2005).

Tire wear particles (TWPs) are produced by the shear force between the tire tread and road surface. The tire contains natural rubber copolymers such as styrene-butadiene rubber and polyisoprene rubber. Zinc oxide (ZnO) and organic zinc compounds are added to the tire to promote the vulcanization process. There are two methods to study tire wear particles, including laboratory simulations and on-board experiments. Laboratory simulation (Dall'osto et al., 2014; Kim and Lee, 2018; Park et al., 2018) simulates the tire wear of a vehicle during driving on an actual road through the friction encountered between the tire and road surface. The on-board experiment can be used to collect the sample behind the vehicle tire. The tire wear sample is collected as the vehicle drives on the actual road. Apeagyei et al. (2011) found that the Zn in TWPs is 13 times that of brake pad wear. Dahl et al. (2006) used a VTI road simulator to study ultrafine particles in TWPs and found that the average diameter of TWPs is 15–50 nm. Mathissen et al. (2011) analyzed the characteristics of ultrafine particle emissions from tire and surface wear via EEPS (TSI Incorporated) installation and found particulate production in the size range of 6–562 nm. The emission will significantly increase when tires side slip. Dall'osto et al. (2014) used a tire wear test platform and particle size spectrometer (APS & SMPS, TSI Incorporated) to detect the particle size distribution of particles in the range of 6–20 μm and found peaks at 35 nm and 85 nm.

In conclusion, previous vehicle non-exhaust emissions studies have mainly used traditional sampling and testing equipment, including ELPI, EEPS, APS and SMPS. In recent years, with the development of science and technology, a variety of advanced high-resolution analytical technology equipment has emerged. Single-particle mass spectrometry has many unique advantages over traditional particulate matter analysis methods (Pratt and Prather, 2012). First, single-particle mass spectrometry is a real-time sampling technique that does not require complex preprocessing of the analyzed samples. Second, the particle size of single particles and the corresponding chemical composition can be analyzed simultaneously. In addition, single particle mass

spectrometry technology usually utilizes high-energy pulsed lasers as the ionization source, which can resolve and ionize almost all types of particles. Li et al. (2014) used single particle aerosol mass spectrometer (SPAMS) to study the composition and source of aerosols under sand and dust storms conditions in Beijing for the first time. Bi et al. (2011) studied biomass combustion in the Pearl River Delta region using SPAMS. Tao et al. (2011) studied the aerosol characteristics during the Shanghai World Expo with SPAMS in two different weathers. Zhang et al. (2009) used SPAMS to study the characteristics and possible sources of lead in the atmosphere of Shanghai.

The single-particle aerosol research results of brake wear particles (Beddows et al., 2016) show strong signal peaks for Fe, FeO_2, Ba and BaO. Previous studies have found that brake pad wear particles in urban atmospheric environments are detected less frequently (1 %–10 %) via the brake pad wear characteristics m/z search method. The main tracer compounds of tire wear include PAHs, benzothiazole (Zhang et al., 2018) and metal elements (Adachi and Tainosho, 2004). The Zn elements in road dust are usually mainly arise from tire wear (Adachi and Tainosho, 2004) since Zn usually accounts for approximately 1 % (Councell et al., 2004) of the tire quality. Single particle aerosol spectrometry of tire wear particles (Dall'osto et al., 2014) has shown potassium or organic signal peaks (m/z = 39), sulphur aromatic peaks (m/z = 69,81,95), and the Zn peaks (m/z = 64). Pure tire wear particles are not common in real-world road dust samples and environmental aerosols. In contrast, tire wear particles are mostly mixed with crust minerals and other substances (such as Li, Na, Ca, Fe, Sb, and phosphate), possibly including lubricants and plant debris. Previous studies searching for the proportion of tire wear particle characteristic at roadside sites have found that tire wear particles contribute approximately 2 % of the total environmental particles.

Tianjin is an international shipping centre and logistics centre in northern China. With the rapid development of economic and social development, the traffic demand in Tianjin is indicating a trend of continuous improvement. Tianjin Port, located in the core area of Tianjin Binhai New Area, has become the seventh largest port in China (the largest port in the Beijing-Tianjin-Hebei region). The logistics traffic (mainly heavy diesel trucks) entering and leaving the port area is growing rapidly. Heavy diesel trucks make up a higher percentage of the fleet in central urban areas. The impact of heavy-duty diesel vehicle emissions on the surrounding air quality cannot be ignored. Meanwhile, due to the heavier weight of heavy-duty diesel vehicles, there may be more brake pad wear emissions and tire wear emissions during driving. Therefore, to accurately quantify the contribution of vehicle fleet emissions to particulate matter in the roadside environment, an SPAMS was used to conduct sampling tests for typical entry and exit highways in Tianjin Port. The SPAMS data were processed and analyzed by the PMF method. Finally, the contribution of each source class to the particulate matter in the roadside environment was obtained.

2 Materials and methods

2.1 Sampling information

Continuous on-site monitoring of TEDA Street was carried out from October 24 to November 12, 2018. The roadside monitoring site was located at the intersection of TEDA Street and Huayuan Street (39°01′56.92″N, 117°42′12.83″E).

2.2 Sampling equipment

A single particle aerosol mass spectrometer (SPAMS-0515, Guangzhou Hexin Instrument Co. Ltd. China) was used to continuously observe the particle size and chemical composition information of the atmospheric particulates at the roadside. A Pegasor AQTM Urban (PAQU, Pegasor.Oy) was used for online monitoring of $PM_{2.5}$. An AethalometerTM black carbon meter (AE 33, Magee Technology Corporation, USA) was used for real-time monitoring of black carbon aerosols. The time resolution of these pollutant detection devices was 1 second.

An automatic weather station VAISALA WXT520 (Vaisala Oyj) was used to observe meteorological parameters (temperature, relative humidity, wind speed, wind direction, atmospheric pressure). The time resolution for the meteorological data collection in this study was 1 minute.

Traffic lidar (UMRR Traffic Management Sensor, smartmicro, Germany) was used to monitor the traffic flow. The traffic lidar instrument was installed on the overpass of TEDA Street. The wide beams from lidar can cover all lanes and record the passing vehicles via multitarget tracking technology. The traffic volume, speed, and vehicle length on the road were recorded. The licence plate data for vehicles were captured by a Hikvision high-definition network machine and used to identify vehicle emission standard information.

2.3 Data analysis

2.3.1 SPAMS data processing

The maximum external trigger pulse frequency of SPAMS is 20 Hz, so the maximum number of ionized particles per second is 20. Continuous online observation will generate huge datasets. Two analysis methods are mainly used: the characteristic ion method and algorithm

clustering. The characteristic ion method extracts a certain type of particulate matter with one or more characteristic component ion fragments and defines it as a certain type. Algorithm clustering can use various algorithms to group particles with similar characteristics in the mass spectrum. The ART-2a algorithm was used to perform cluster analysis in this study. ART-2a is an adaptive resonance algorithm based on neural networks and is widely used in single particle mass spectrometry data analysis.

The ART-2a method screens and determines the same type of particulate matter by adjusting the alert factor and learning efficiency. The higher the alert factor, the smaller the difference in particulate matter within the same category, but the total number of categories will increase. Considering the similarity of particles and the total number of categories, the alert factor was selected to be 0.65, and the learning efficiency was 0.05. COCO software under the MATLAB platform was used for SPAMS data processing.

2.3.2 Positive matrix factorisation (PMF)

The EPA PMF V5.0 model was used to analyze the source of the single-particle aerosol mass spectrometry data. The PMF model decomposes the receptor data based on the least squares method to obtain the source component matrix and the source contribution matrix (Gong et al., 2012; Wen et al., 2016). The PMF model uses multivariate analysis of chemical species concentrations and their uncertainty determined from the weighted least square method to resolve the potential sources (Paatero and Tapper, 1994). The formula can be expressed as follows:

$$X_{ij} = \sum_{k=1}^{p} g_{ik} f_{kj} + e_{ij}, \quad (1)$$

where X_{ij} is the measured concentration of the jth element in the ith sample; g_{ik} is the contribution of the kth pollution source for the ith sample; f_{kj} is the concentration of the jth element in the kth pollution source; e_{ij} is the residual term, the difference between the measured value and estimated value; p is the number of factors; i is the number of PM samples; j is the number of elements; and k is the number of pollution sources.

3 Results and discussion

3.1 Vehicle activity and meteorological condition

As an important transportation channel for Tianjin Port, TEDA Street has undertaken numerous logistics and living transportation needs in the core area of Binhai New Area. Fig. 1 shows vehicle fleet composition during the test.

The average daily traffic flow and average speed on TEDA Street are 15907 ± 2235 vehicles and 58.8 km/h, respectively. Similar to the traffic characteristics of typical urban roads, the daily trend for traffic flow and speed on TEDA Street also shows obvious “M” and “W” characteristics. In addition, the traffic flow on TEDA Street on weekdays also shows a significant “tidal traffic” feature. In the morning, people drive into the Tianjin port area for production activities. Therefore, the traffic volume in the morning peak is significantly higher than that in the evening peak.

Through analysis of the vehicle licence plate data, detailed information for the TEDA Street fleet composition can be finally obtained, including fuel type (gasoline, diesel and new energy), emission standards (from China I to China V), and vehicle types (small passenger cars, medium passenger cars, large passenger cars, light trucks, medium trucks and large trucks).

Fig. 1 shows that small passenger cars (63 %), light trucks (21 %) and large trucks (10 %) and are the three major types of vehicles using TEDA Street. Gasoline vehicles, diesel vehicles and new energy vehicles account for 84 %, 13 % and 3 % of the mixed fleet, respectively. The emission standard for the mixed fleet is mainly China IV (45 %), followed by China V (34.7 %), China III (17.9 %), China II (1.9 %), and China I (0.5 %).

In addition, based on video recording and manual screening, non-local licence trucks account for 59 % of all trucks in TEDA Street, which represents a high level of activity. In view of the gap between the fuel quality, I/M level and post processing technology of non-local trucks and local vehicles, the management and law enforcement of non-local high-emission trucks should be given sufficient attention.

The meteorological conditions at the roadside during the sampling time are shown in Fig. 2. The temperatures are 12.1 ± 4.0 °C, from 3.7 °C to 21.8 °C. The recorded wind speed during the sampling periods was approximately 0.14–3.82 m/s. RH is negatively correlated with temperature. There was a significant rainfall event during the test, which may have caused the instrumental data to be biased.

3.2 SPAMS characteristics

During the test period, 6.3 million particles were captured via the SPAMS, including 1.3 million particles with positive and negative spectral map information. A total of 734 categories were identified by clustering the top 90 % of the data using the ART-2a method. Finally, after manual identification, 10 categories were combined, including heavy metal (HM), high molecular organic carbon (HOC), organic carbon (OC), mixed carbon (ECOC), elemental carbon (EC), rich potassium (K), levofloxacin-rotation glucose (LEV), rich Na (Na), SiO_3 and others categories (Fig. 2). The average spectrum of each category is shown in Figs. S1–S9.

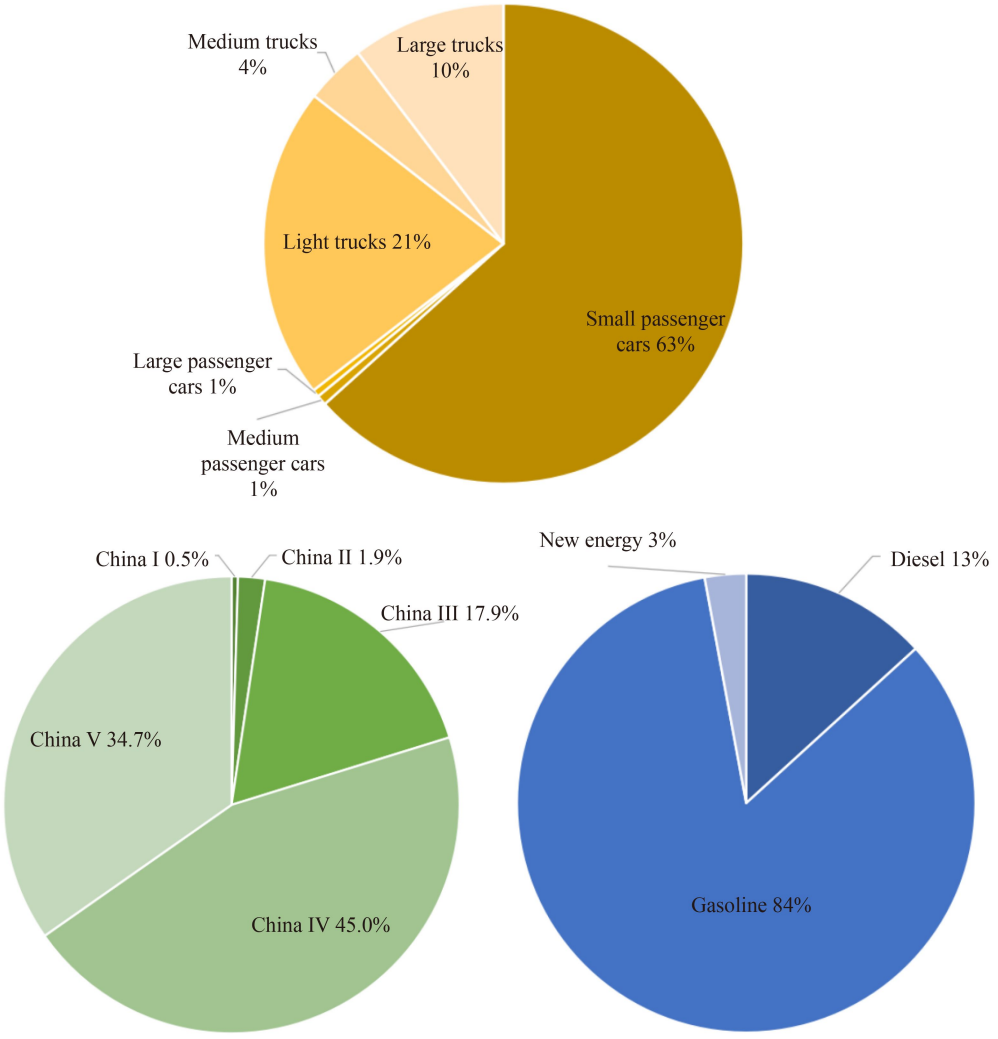

Fig. 1 Vehicle fleet composition during the test.

Fig. S1 shows the mass spectrum peak characteristics of heavy metal elements, including Fe^+ (*m/z* = 56), Cu^+ (*m/z* = 64), and Pb^+ (*m/z* = 206, 207, 208). Fig. S2 shows the mass spectrum peak characteristics of the HOC particles. In addition to low molecular organic carbon with m/z ratios of 27, 37, 43, 51, 63, HOC also includes high molecular organic carbon signals with *m/z* ratios ranging between 100–240, such as 149 ($C_{12}H^+$), 163 ($C_{13}H^+$), 165 ($C_{13}H^+$), 178 ($C_{14}H^+$), 189 ($C_{15}H^+$), 202 ($C_{16}H^+$), and 228 ($C_{17}H^+$) signal peaks. Fig. S3 shows the mass spectrum peak characteristics of the OC particles. The positive spectrum of OC particles contains common OC carbon peaks with m/z ratios of 27, 37, 43, 51, and 63. In addition, the spectrum shows rich nitrates (*m/z* = 46, 62) and sulphates (*m/z* = 80, 97), indicating that the OC particles undergo a certain ageing process. Figure S4 shows the mass spectrum peak characteristics of ECOC particles. ECOC particles contain a series of elemental carbon peaks and organic carbon peaks, such as C_2H^+ (*m/z* = 27), C_3H^+ (*m/z* = 37), and $C_2H_3O^+/C_2H_5N^+$ (*m/z* = 43). The most obvious feature of ECOC is that the particulate matter peaks occur at both *m/z* = 36 and *m/z* = 37, and the signal intensities of the two peaks are similar. Fig. S5 shows the mass spectrum peak characteristics of EC particles. Both the positive and negative spectra measured for the EC particles contain a series of elemental carbon mass peaks (*m/z* = 12, 36, 48, 60). The negative spectrum contains nitrate (*m/z* = 46, 62) and sulphate (*m/z* = 97). Figs. S6 and S7 show K-rich particles and Na-rich particles, respectively. The mass spectrum peaks are characterized by the positive spectra for the K-ion peak (*m/z* = 39) and Na-ion peak (*m/z* = 23). The signal is significantly stronger than the other signal peaks. The negative spectrum mainly shows secondary ions, including nitrate (*m/z* = 46, 62) and HSO_4^- (*m/z* = 97). In addition, the negative spectrum of K-rich particles also contains CN^- peaks (*m/z* = –26). Fig. S8 shows levoglucose particles, which usually contain the K_2SO^+ peak (*m/z* = 213) and fragment peaks produced by cellulose pyrolysis (CN^- and CHO^-). Fig. S9 shows the mass spectrum peak characteristics of SiO_3. The positive spectrum also shows a Fe-ion peak (*m/z* = 56). The

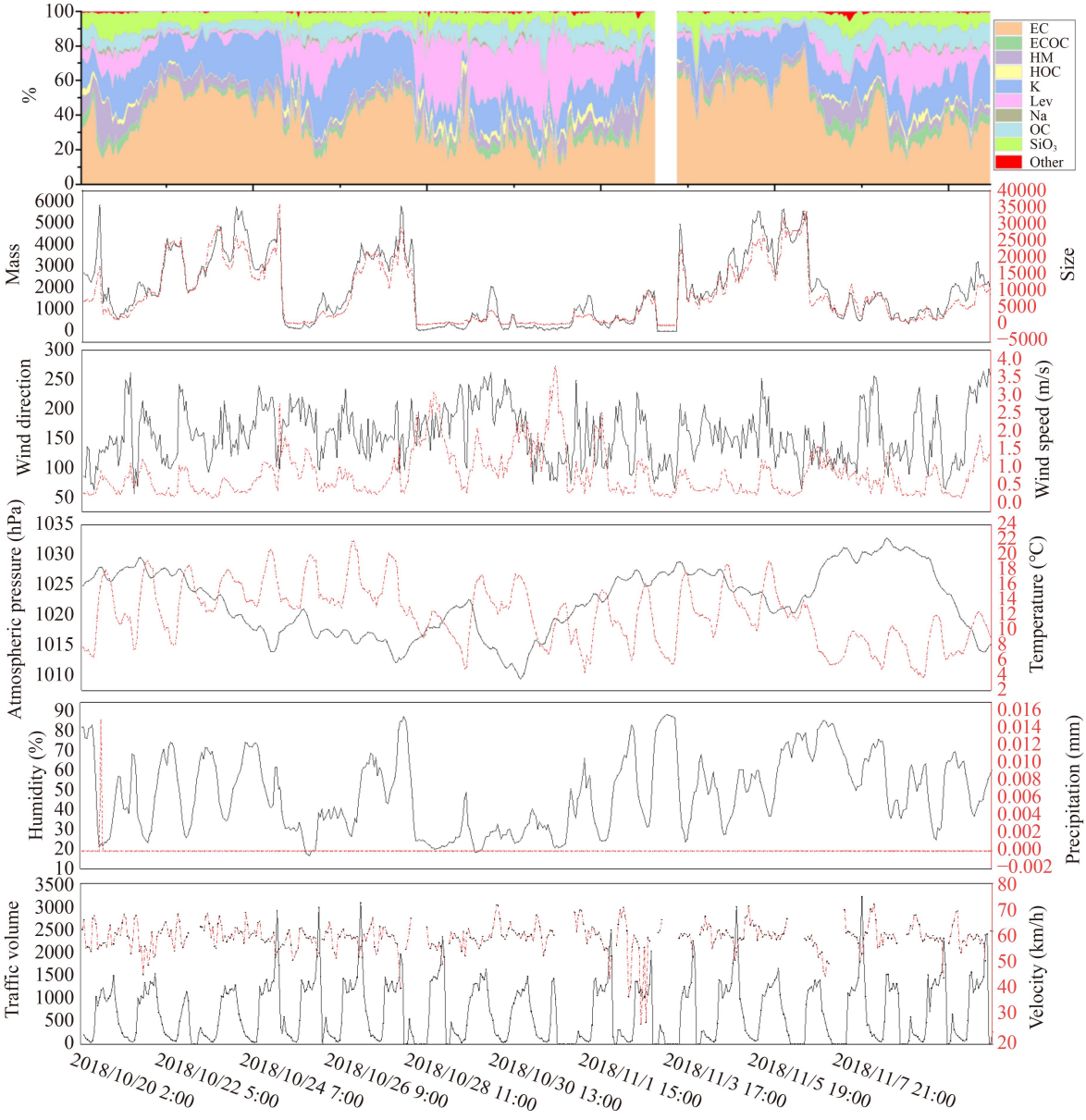

Fig. 2 SPAMS component map, meteorological parameters, and traffic flow distribution characteristics during the test period.

negative spectrum contains an obvious (SiO_3^-) peak.

This study compared the correlation between the hourly number/mass concentration of SPAMS data and the hourly mass concentrations of $PM_{2.5}$ and BC (Fig. 3). As shown in Fig. 3, the particle number concentration measured by SPAMS shows a good linear correlation with the mass concentrations of $PM_{2.5}$ and BC, with R^2 reaching 0.504 (Pearson's r is 0.710) and 0.495 (Pearson's r is 0.704), respectively. SPAMS cannot be used to detect the information for particulate matter below 200 nm, which cannot represent the number concentration of particulate matter below $PM_{2.5}$. However, the mass concentration of $PM_{2.5}$ is mainly dominated by particles above 200 nm, so the particle number concentration measured by SPAMS has a certain correlation with the mass concentrations of $PM_{2.5}$ and BC. Therefore, it can be considered that the particulate matter captured by SPAMS can reflect the pollution degree of fine particulate matter to a certain extent.

3.3 Diurnal variation analysis

Fig. 4 shows the average diurnal variation of different chemical components measured by SPAMS, which can reflect the information for potential emission sources. This study includes 15 working days and 6 non-working days, which are basically representative. EC, ECOC, OC, HM and crustal dust components have high values from 7:00–9:00 AM (morning peak), indicating that these chemical components are directly or indirectly related to

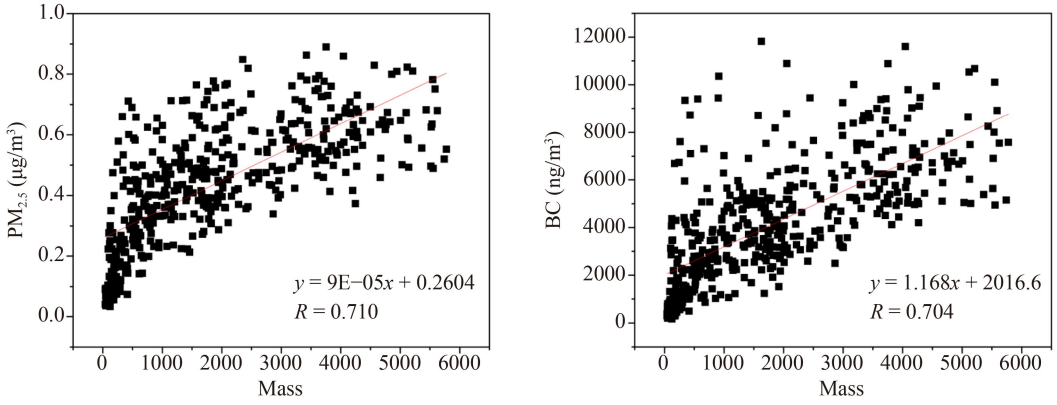

Fig. 3 Correlation between the hourly concentration of SPAMS and the hourly level of $PM_{2.5}$ and BC.

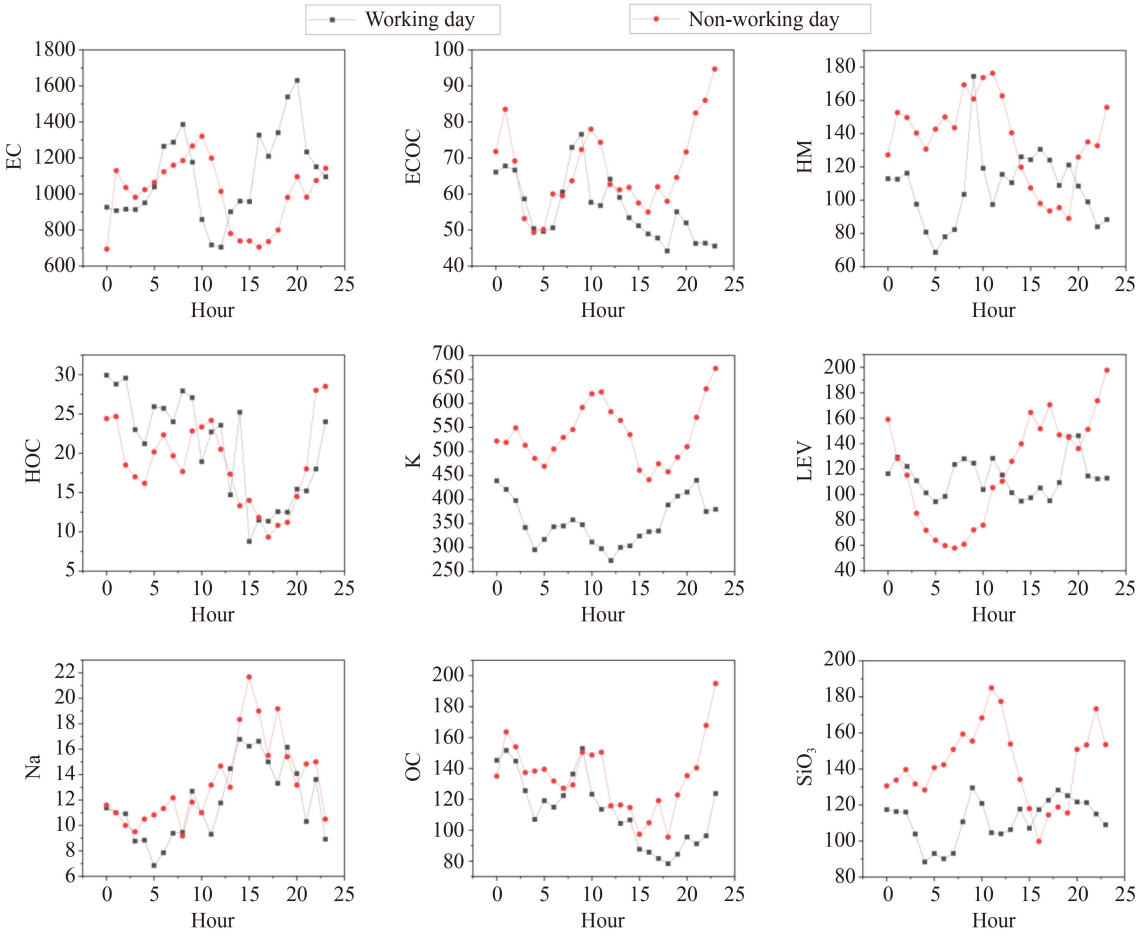

Fig. 4 Average diurnal variation in different chemical components measured by SPAMS.

vehicle emissions. Crustal dust in the roadside environment can be mainly contributed by road dust generated by motor vehicle activities. The roadside environment is affected by vehicle emissions during the morning peak hours. LEV and Na present a unimodal distribution with high values at 15:00–18:00. The reason may be related to the strong biomass combustion emissions produced during this period.

Fig. 5 shows the diurnal trend for some metal elements, ions and organics on working days and non-working days. This study analyses the chemical components related to vehicle non-exhaust emissions (brake pad wear and tire wear), including Cu, Fe, Sb, Zn, Pb, V, Ni, sulphate ions, nitrate ions, phosphate ions, chloride ions and sulphur-containing aromatic hydrocarbons.

As shown in Fig. 5, the metal elements (Cu, Sb, Zn and

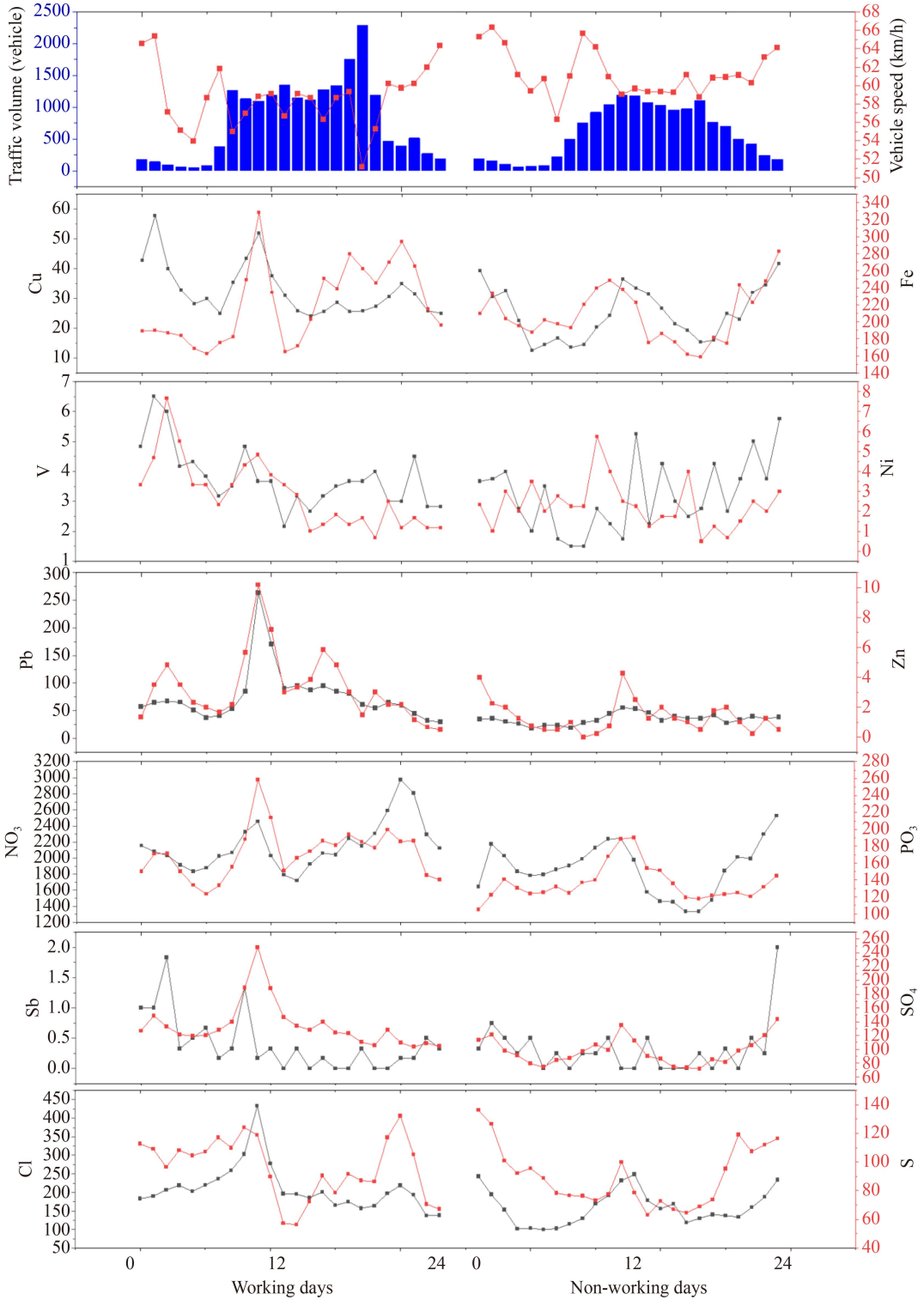

Fig. 5 Diurnal variation characteristics of traffic flow, speed, Cu, Fe, Sb, Zn, Pb, V, Ni, sulphate ions, nitrate ions, phosphate ions, chloride ions and sulphur-containing aromatic hydrocarbons on working days and non-working days.

Pb), sulphur-containing aromatic hydrocarbons and polycyclic aromatic hydrocarbons in the roadside environment all show the characteristics of a morning peak for the working day, indicating that they are affected by the high vehicle flow rate. Cu, Zn, V and sulphur-containing aromatic hydrocarbons show high concentrations at night, which may be related to heavy diesel vehicles. Secondary ions such as sulphate, nitrate,

phosphate and chloride ions also show high concentrations at night, which may be related to the stable weather conditions and the high compression of the mixed layer at night.

Overall, the SPAMS data can reflect diurnal trends in each chemical component. The daily variation characteristics of the non-exhaust particulate matter of motor vehicles can be obtained by combining the diurnal change characteristics of these chemical components and the identifiable components of non-exhaust emission particles, which is conducive to the further verification of the source analysis results.

3.4 Source analysis

The input data for the PMF model are the mass concentration data and uncertainty data obtained from the SPAMS data. The value of Q true/Q expected is shown in Table S1. As shown in Table S1, 5 to 9 factors were calculated. The corresponding Q(Robust)/Q(Expected) values were determined to be 10.755, 9.588, 8.688, 8.027 and 7.070, and the ΔQ(Robust)/Q(Expected) values were 1.167, 0.900, 0.661 and 0.957, respectively. The value of ΔQ (Robust)/Q(Expected) obtained from 7 to 8 factors was the smallest (0.661), and 8 factors were resolved by the PMF model. The source profile of each factor obtained by the PMF model simulation is shown in Fig. 6.

The identification components of factor 1 are EC and OC, so they can be judged to act as a source of motor vehicle emissions. The identification components of factor 2 are V (m/z = 51, 67) and Ni (m/z = 58), as well as the ECOC components, while ship emissions are the main source of V, so factor 2 is identified as ship emissions. The identification components of factor 3 are Pb, Cl and SO_4, which are often thought to be derived from coal-fired sources. This factor also contains sulphate components, so factor 3 is judged to be a coal combustion source. Factor 4 has a distinct CNO^- component for the fragments produced by the heated cracking of L-glucose and cellulose identified as a source of biomass combustion. The identification components of factor 5 include Ca, Mg, Al, and AlO_2, so factor 5 is identified as dust. Factor 6 is characterized by a strong Sb content. Sb can often be used as a marker component of brake pad wear particles, so factor 6 is identified as brake pad wear. Factor 7 is characterized by having a distinct Zn component, so it is identified as tire wear. Factor 8 is characterized by strong OC, ECOC, SO_2, SO_3, and SO_4 components, so it is identified as a coal combustion source.

By comparing the predicted value under the 8-factor PMF analysis scheme with the observed value (Fig. S10), it is found that the PMF predicted value and the measured value have a very good correlation. The coefficient R^2 reaches as high as 0.995, indicating that the 8-factor PMF analysis scheme in this study can be used to better analyze the observed values. Factor 3 and factor 8 are combined to obtain 7 major types of factors. The relative contributions of each factor (Fig. 7) were determined to be 44.8 % for vehicle emission, 14.5 % for coal-fired source, 12.2 % for biomass source, 9.4 % for crustal dust, 9.0 % for ship emission, 6.6 % for tires wear and 3.5 % for brake pads wear.

4 Conclusions

We conducted a long-term roadside sampling tests on typical entry and exit highways in Tianjin Port and obtained the single particle aerosol emission characteristics and traffic fleet information via a single particle aerosol mass spectrometer and traffic lidar. The PMF model is used to analyze the source of the single-particle aerosol mass spectrometry data. The contribution of vehicle fleet emissions to particulate matter in the roadside environment is accurately assessed. The main conclusions of this study include:

1) The average daily traffic flow and average speed on TEDA Street during sampling period are 15907 ± 2235 vehicles and 58.8 km/h, respectively. The daily trend for traffic flow and speed on TEDA Street shows obvious “M” and “W” characteristics. Gasoline vehicles, diesel vehicles and new energy vehicles account for 84 %, 13 % and 3 % of the mixed fleet, respectively. The emission standard for the mixed fleet is mainly China IV (45 %), followed by China V (34.7 %), China III (17.9 %).

2) SPAMS was used to analyze the single particle aerosol emission characteristics at the roadside for three weeks. Heavy metal elements, high molecular organic carbon, organic carbon, mixed carbon, elemental carbon, rich potassium, levofloxacin-rotation glucose, rich Na, SiO_3 and other categories were combined. The particle number concentration measured by SPAMS shows a good linear correlation with the mass concentrations of $PM_{2.5}$ and BC, which can be considered that the SPAMS data reflect the pollution degree of fine particulate matter. The metal elements, sulphur-containing aromatic hydrocarbons and polycyclic aromatic hydrocarbons indicate the characteristics of a morning peak for the working day. Cu, Zn, V and sulphur-containing aromatic hydrocarbons show high concentrations at night, which are related to heavy diesel vehicles.

3) Vehicle exhaust emissions (44.8 %), coal-fired sources (14.5 %), biomass combustion (12.2 %), crustal dust (9.4 %), ship emissions (9.0 %), tires wear (6.6 %) and brake pads wear (3.5 %) were identified as the seven major sources of particulate matter at the roadside. The proportion of non-exhaust particulate matter emissions (including brake pads wear and tires wear) can reach 10.1 % at road environment. With the extensive development of new energy vehicles, the proportion of vehicle exhaust

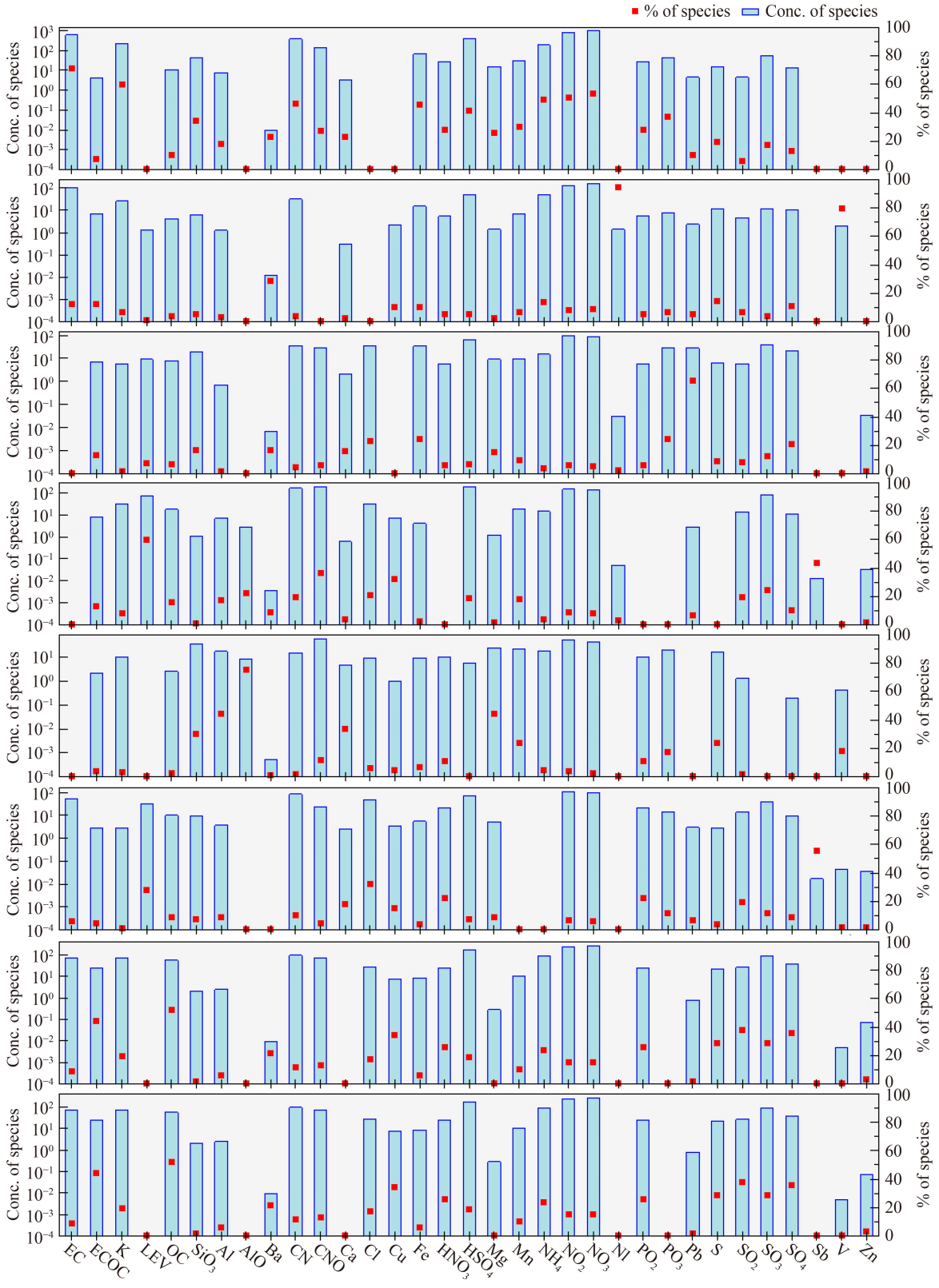

Fig. 6 Source profile of each factor obtained by PMF.

emissions will gradually decrease in the future. Therefore, the research on non-exhaust emission pollutants of vehicles should be paid more attention.

Acknowledgements This work was supported by the National Natural Science Foundation of China (Nos. 42107114 and 42177084), the Tianjin Science and Technology Plan Project (No. 20YFZCSN01000), and the Fundamental Research Funds for the Central Universities (No. 63221411).

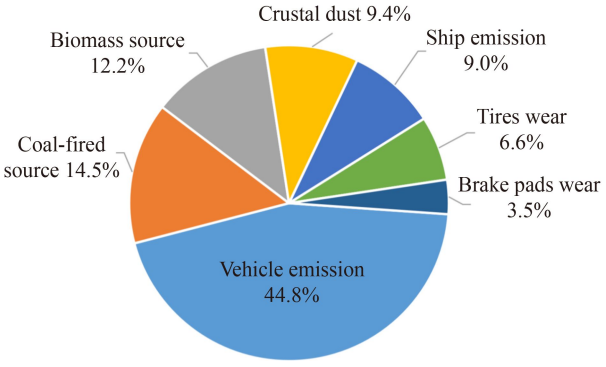

Fig. 7 Contribution ratio of each factor via PMF model.

Electronic Supplementary Material Supplementary material is available in the online version of this article at https://doi.org/10.1007/s11783-023-1662-8 and is accessible for authorized users.

References

Abu-Allaban M, Gillies J A, Gertler A W, Clayton R, Proffitt D (2003). Tailpipe, resuspended road dust, and brake-wear emission factors from on-road vehicles. Atmospheric Environment, 37(37): 5283–5293

Adachi K, Tainosho Y (2004). Characterization of heavy metal particles embedded in tire dust. Environment International, 30(8): 1009–1017

Amato F, Cassee F R, Denier van der Gon H A, Gehrig R, Gustafsson M, Hafner W, Harrison R M, Jozwicka M, Kelly F J, Moreno T, Prevot A S, Schaap M, Sunyer J, Querol X (2014). Urban air quality: the challenge of traffic non-exhaust emissions. Journal of Hazardous Materials, 275: 31–36

Apeagyei E, Bank M S, Spengler J D (2011). Distribution of heavy metals in road dust along an urban-rural gradient in Massachusetts. Atmospheric Environment, 45(13): 2310–2323

Baensch-Baltruschat B, Kocher B, Stock F, Reifferscheid G (2020). Tyre and road wear particles (TRWP): a review of generation, properties, emissions, human health risk, ecotoxicity, and fate in the environment. Science of the Total Environment, 733: 137823

Beddows D C S, Dall'osto M, Olatunbosun O A, Harrison R M (2016). Detection of brake wear aerosols by aerosol time-of-flight mass spectrometry. Atmospheric Environment, 129: 167–175

Bi X, Zhang G, Li L, Wang X, Li M, Sheng G, Fu J, Zhou Z (2011). Mixing state of biomass burning particles by single particle aerosol mass spectrometer in the urban area of PRD, China. Atmospheric Environment, 45(20): 3447–3453

Councell T B, Duckenfield K U, Landa E R, Callender E (2004). Tire-wear particles as a source of zinc to the environment. Environmental Science & Technology, 38(15): 4206–4214

Dahl A, Gharibi A, Swietlicki E, Gudmundsson A, Bohgard M, Ljungman A, Blomqvist G, Gustafsson M (2006). Traffic-generated emissions of ultrafine particles from pavement-tire interface. Atmospheric Environment, 40(7): 1314–1323

Dall'Osto M, Beddows D C S, Gietl J K, Olatunbosun O A, Yang X, Harrison R M (2014). Characteristics of tyre dust in polluted air: studies by single particle mass spectrometry (ATOFMS). Atmospheric Environment, 94: 224–230

Garg B D, Cadle S H, Mulawa P A, Groblicki P J, Laroo C, Parr G A (2000). Brake wear particulate matter emissions. Environmental Science & Technology, 34(21): 4463–4469

Gasser M, Riediker M, Mueller L, Perrenoud A, Blank F, Gehr P, Rothen-Rutishauser B (2009). Toxic effects of brake wear particles on epithelial lung cells in vitro. Particle and Fibre Toxicology, 6(1): 30–42

Gong Z, Lan Z, Xue L, Zeng L, He L, Huang X (2012). Characterization of submicron aerosols in the urban outflow of the central Pearl River Delta region of China. Frontiers of Environmental Science & Engineering, 6(5): 725–733

Grieshop A P, Lipsky E M, Pekney N J, Takahama S, Robinson A L (2006). Fine particle emission factors from vehicles in a highway tunnel: effects of fleet composition and season. Atmospheric Environment, 40: 287–298

Kim G, Lee S (2018). Characteristics of tire wear particles generated by a tire simulator under various driving conditions. Environmental Science & Technology, 52(21): 12153–12161

Kwak J H, Kim H, Lee J, Lee S (2013). Characterization of non-exhaust coarse and fine particles from on-road driving and laboratory measurements. Science of the Total Environment, 458-460: 273–282

Li L, Li M, Huang Z, Gao W, Nian H, Fu Z, Gao J, Chai F, Zhou Z (2014). Ambient particle characterization by single particle aerosol mass spectrometry in an urban area of Beijing. Atmospheric Environment, 94: 323–331

Masclans Abello P, Medina Iglesias V, De Los Santos Lopez M A, Alvarez-Florez J (2021). Real drive cycles analysis by ordered power methodology applied to fuel consumption, CO_2, NO_x and PM emissions estimation. Frontiers of Environmental Science & Engineering, 15(1): 4

Mathissen M, Scheer V, Vogt R, Benter T (2011). Investigation on the potential generation of ultrafine particles from the tire-road interface. Atmospheric Environment, 45(34): 6172–6179

Paatero P, Tapper U (1994). Positive matrix factorization: a non - negative factor model with optimal utilization of error estimates of data values. Environmetrics, 5(2): 111–126

Pant P, Harrison R M (2013). Estimation of the contribution of road traffic emissions to particulate matter concentrations from field measurements: a review. Atmospheric Environment, 77: 78–97

Park I, Kim H, Lee S (2018). Characteristics of tire wear particles generated in a laboratory simulation of tire/road contact conditions. Journal of Aerosol Science, 124: 30–40

Pratico F G, Briante P G (2020). Particulate Matter from Non-exhaust Sources. Vilnius: Lithuania

Pratt K A, Prather K A (2012). Mass spectrometry of atmospheric aerosols-recent developments and applications. Part II: on-line mass spectrometry techniques. Mass Spectrometry Reviews, 31(1): 17–48

Roubicek V, Raclavska H, Juchelkova D, Filip P (2008). Wear and environmental aspects of composite materials for automotive braking industry. Wear, 265(1–2): 167–175

Tao S, Wang X, Chen H, Yang X, Li M, Li L, Zhou Z (2011). Single particle analysis of ambient aerosols in Shanghai during the World

Exposition, 2010: two case studies. Frontiers of Environmental Science & Engineering, 5(3): 391–401

Timmers V R J H, Achten P A J (2016). Non-exhaust PM emissions from electric vehicles. Atmospheric Environment, 134: 10–17

von Uexkull O, Skerfving S, Doyle R, Braungart M (2005). Antimony in brake pads: a carcinogenic component? Journal of Cleaner Production, 13(1): 19–31

Wen W, Cheng S, Liu L, Wang G, Wang X (2016). Source apportionment of $PM_{2.5}$ in Tangshan, China: hybrid approaches for primary and secondary species apportionment. Frontiers of Environmental Science & Engineering, 10(5): 6

Yue X, Wu Y, Huang X, Ma Y, Pang Y, Bao X, Hao J (2012). Impact of gasoline engine deposits on light duty vehicle emissions: in-use case study in Beijing, China. Frontiers of Environmental Science & Engineering, 6(5): 717–724

Zhang J, Zhang X, Wu L, Wang T, Zhao J, Zhang Y, Men Z, Mao H (2018). Occurrence of benzothiazole and its derivates in tire wear, road dust, and roadside soil. Chemosphere, 201: 310–317

Zhang Y, Wang X, Chen H, Yang X, Chen J, Allen J O (2009). Source apportionment of lead-containing aerosol particles in Shanghai using single particle mass spectrometry. Chemosphere, 74(4): 501–507

Zhu R, Hu J, He L, Zu L, Bao X, Lai Y, Su S (2021). Effects of ambient temperature on regulated gaseous and particulate emissions from gasoline-, E10- and M15-fueled vehicles. Frontiers of Environmental Science & Engineering, 15(1): 14